Relaxation processes in coherent-population trapping

Ennio Arimondo*
JILA, University of Colorado, Campus Box 440, Boulder, Colorado 80309-0440
(Received 31 October 1995)

The role played by a buffer gas in the ground-state superposition created in coherent-population-trapping experiments is investigated theoretically. The density matrix equations are solved on the basis of the coupled-noncoupled states. The velocity-changing collisions are examined in the limit of strong collisions. The relaxation rate for transfer of the ground-state superposition between atoms with different velocities is derived from a fit of available experimental results. [S1050-2947(96)02708-4]

PACS number(s): 32.80.Bx, 34.50.−s, 42.55.−f, 34.10.+x

I. INTRODUCTION

Coherent-population trapping in a three-level Λ system is based on the preparation of atoms in a coherent superposition of the two lower states. Owing to quantum interferences in the absorption of two lasers exciting the lower states to the upper state, the trapping superposition is electromagnetically transparent, i.e., it does not absorb the incoming laser radiation [1–3]. Atomic preparation in a nonabsorbing superposition has applications in light-induced drift, laser cooling, laser without inversion, adiabatic transfer, and so on [4]. The preparation of the atomic superposition requires a long interaction time, and its use imposes a preservation of the coherent superposition in atomic collisions. Experiments in the context of light-induced drift have examined the relaxation processes affecting the atomic superposition of sodium hyperfine ground states [5]. In experiments involving laser without inversion, the dependence on collisions for a sodium atomic superposition was measured and found surprisingly sensitive to buffer-gas pressure [6]. The effects of atomic collisions on these last experiments was examined theoretically, including the important role played by velocity-changing collisions (VCC) [7]. Additional measurements for preparation of sodium atoms into coherent-population trapping at large pressures of buffer-gas have been performed recently by Xu [8], with a dependence on the buffer-gas pressure quite different from that reported in the laser-without-inversion experiments: the coherent-population-trapping signal was found to be weakly sensitive to buffer-gas pressure. The different dependence on the buffer gas in the two investigations was explained in Ref. [7] in terms of optical pumping between the Zeeman ground levels. Because of a different polarization geometry in the laser-without-inversion experiment, optical pumping depleted the levels of the coherent superposition, whereas in Refs. [1,3,8] optical pumping enhanced the occupation of the coherent superposition atomic levels.

The results of Ref. [8] demonstrate that a large coherent atomic superposition of sodium hyperfine ground states may be produced for operation in the presence of a buffer gas. As a consequence, it is important to investigate more carefully the relaxation processes affecting that superposition. The present theoretical analysis examines atomic coherent-trapping superposition in the presence of different sources of relaxation: the interaction time defined by the atomic time of flight through the laser beam, the collisional damping of the atomic polarizations and of the coherences, and VCC. By making use of available rates for the collisional relaxation of polarizations and for VCC, we derive a value for the collisional relaxation of the coherent superposition of the sodium hyperfine ground states from a fit of the data of Ref. [8].

The experiments of Refs. [1,8] were performed in a sodium vapor cell with helium as a buffer gas. Two phase-correlated laser fields, copropagating through the sodium cell at an angle with an applied magnetic field, linearly and circularly polarized, coupled the ground-state pair $|3S_{1/2};F=2;m_F=2\rangle$, $|3S_{1/2};F=1;m_F=1\rangle$, respectively, to a common level of the $3P_{1/2}$ excited state. Therefore population trapping was created via atomic coherence between a pair of ground-state hyperfine levels. The coherent-population-trapping preparation was monitored as a decrease in the fluorescent light emitted by the sodium atoms. As pointed out by Ref. [5], a sodium hyperfine ground-state-coherent superposition is quite robust against collisions because the two sodium ground states involved in the superposition experience a common shift in collisions with a buffer gas. Thus a very large number of collisions with the buffer gas is required to destroy the ground-state coherence. The analysis presented in this work evidences that velocity-changing collisions transfer efficiently between different velocity classes the coherent superposition prepared by the laser. The laser copropagating geometry applied in the experiments of Refs. [1,8], as well as in those of light-induced drift [5] and laser without inversion [6], allows a preparation of coherent-population trapping for all the velocity classes. On the contrary, a laser counterpropagating geometry produces a velocity-selective coherent-population trapping, as in Ref. [9].

The phenomenon of coherent-population trapping is described by differential density matrix equations, as presented in Refs. [2,3]. In the recent work by Graf *et al.* [7], those equations have been written in an integro-differential form to include VCC processes. The relaxation processes produced by collisions with the walls and other atoms may be introduced through use of the coupled and noncoupled linear superposition of ground states defined in Ref. [9]. Solutions of

*Permanent address: Dipartimento di Fisica, Universitá di Pisa, I-56126 Pisa, Italy.

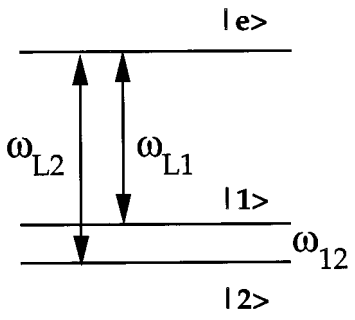

FIG. 1. Schematic representation of the three-level system examined in the coherent-population-trapping experiments of Refs. [1,8].

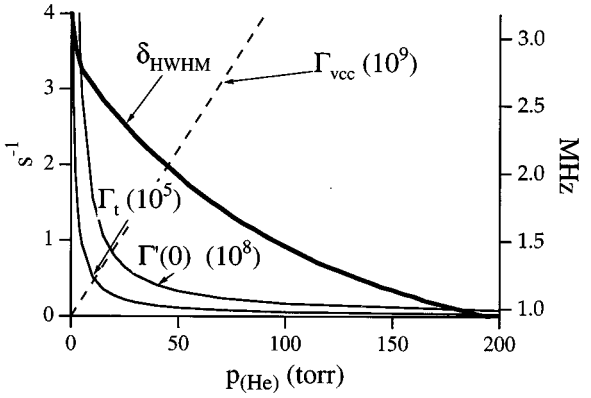

FIG. 2. Ground-state relaxation rates Γ_t, $\Gamma'(0)$, and Γ_{VCC} for atom and laser parameters of the experiment by Xu [8]: $R=0.075$ cm, $T=300$ K, and $\Omega_R=6\Gamma_{\mathrm{sp}}$. Half-width at half maximum δ_{HWHM}, in MHz on the right-hand scale, versus the buffer-gas pressure, derived in the VCC treatment, with ground-state collisional rate chosen to provide the best fit for the dependence of the measured contrast C on the helium pressure.

the density matrix equations in the coupled-noncoupled basis are presented here. The integro-differential equations describing VCC are solved analytically in the hypothesis of very fast collisions thermalizing the ground-state velocity distribution. This approach, introduced in Refs. [10–14] for rate equations of a three-level Λ system, is here extended to the equations with coherences in order to describe the influence of VCC on coherent-population trapping.

The collisional phenomena investigated here are not relevant for the laser cooling process based on the velocity-selective coherent-population trapping, i.e., on the preparation of the atoms on a noncoupled linear superposition of the ground state, more precisely the linear superposition corresponding to zero velocity. In effect the laser cooling experiments are performed in atomic samples at very low density where the collisional rates are very small. On the contrary the phenomenon of reabsorption, i.e., the destruction of the noncoupled superposition of states by the reabsorption of the light emitted by other atoms, is much more important for the lifetime of the noncoupled superposition. This process is briefly discussed in the conclusions and its rate compared to the collisional rates examined in this work.

II. ANALYSIS

A. Density matrix equations

Figure 1 reports a simplified model for the three-level sodium system, to be used in the present theoretical analysis, where $|1\rangle$, $|2\rangle$ stand for the pair of levels within the hyperfine split $3S_{1/2}$ sodium ground-state, coupled by the laser fields to the common excited level $|e\rangle$ within the $3P_{1/2}$ manifold. The atomic energies are defined through the ground-state splitting $\hbar\omega_{12}$, and the energy separation from the excited state to the lower levels, $\hbar\omega_{ei}$ $(i=1,2)$. Each laser beam, frequency ω_{Li}, and electric field amplitude E_{Li} $(i=1,2)$ excites selectively one optical transition, the selectivity being provided by polarization selection rules. For simplicity, the combination of electric field amplitudes and dipole moments d_{ie} is supposed to produce Rabi frequencies equal for the two optical transitions, $\Omega_R=d_{1e}E_{Li}/\hbar=d_{2e}E_{L2}/\hbar$. The wave numbers of the two lasers will be approximated by a single k value. The spontaneous emission decay from $|e\rangle$ is supposed to transfer atoms to the ground states with equal decay rate $\Gamma_{\mathrm{sp}}/2$. This simple model does not include several additional features present in the sodium experiment of Refs. [1,8], such as the different dipole moments on the two transitions and the presence of several hyperfine and Zeeman sublevels. However, the present simple analysis allows the main features of the relaxation processes to be described. The restriction to only two ground states is a good approximation if the optical pumping process transfers all the population to a few states, for instance, $|3S_{1/2},F=2,m_F=2\rangle$ and $|3S_{1/2},F=1,m_F=1\rangle$ using σ^+ polarized light.

The relaxation rate $\Gamma_\perp$ of the optical coherences in the density matrix, $\rho_{e,1}$ and $\rho_{e,2}$, and their complex conjugates, is determined by the spontaneous emission decay Γ_{sp} and by the dephasing collisional rate $\Gamma_\perp^p$,

$$\Gamma_\perp=\frac{\Gamma_{\mathrm{sp}}}{2}+\Gamma_\perp^p. \tag{1}$$

The dephasing rate for sodium-helium collisions reported in Ref. [15] has the value $\Gamma_\perp(\mathrm{Na\text{-}He})=4.16\times10^7\ p\ \mathrm{s}^{-1}\ \mathrm{torr}^{-1}$, where p is the helium pressure. The ground-state relaxation is determined by the transit time rate Γ_t of atoms across the laser beam, with sodium atoms in the laser interaction region replaced by fresh atoms arriving from the volume outside that region. Γ_t depends on the pressure p of the buffer gas and on the sodium diffusion coefficient D_g through a standard relation [16,17]

$$\Gamma_t=2.405^2\frac{D_g}{R^2}\frac{1}{1+c\lambda/R}, \tag{2}$$

where 2.405 is the lowest zero of the zeroth-order Bessel function, λ is the mean free path, R is the radius of the laser beam, and c is a numerical constant equal to 6.8 for a hard-sphere interaction [16]. For sodium atoms diffusing in helium the following values are derived from Ref. [15]: $D_g=555/p\ \mathrm{cm}^2\ \mathrm{s}^{-1}\ \mathrm{torr}^{-1}$ at $T=300$ K, and $\lambda=11.1\times10^{-3}/p\ \mathrm{cm\ torr}^{-1}$. The escape rate Γ_t for sodium in helium is plotted versus the buffer-gas pressure in Fig. 2, for parameters corresponding to Ref. [8]. The collisional decay

$\Gamma_{\rm coh}$ of the ground-state coherence $\rho_{1,2}$ is given by the transit time Γ_t and an additional collisional term $\Gamma^p_{\rm coh}$ proportional to the helium pressure to be derived from a fit of the experimental results

$$\Gamma_{\rm coh}=\Gamma_t+\Gamma^p_{\rm coh}. \tag{3}$$

With the parameters introduced above, the evolution equations of the density matrix equations $\rho(v)$ for atoms with velocity v may be written in the following form [2]:

$$\dot\rho_{1,1}(v)=\frac{\Gamma_{\rm sp}}{2}\rho_{e,e}(v)-\Omega_R{\rm Im}[\tilde\rho_{e,1}(v)]-\Gamma_t\left[\rho_{1,1}(v)-\frac{1}{2}\right], \tag{4a}$$

$$\dot\rho_{2,2}(v)=\frac{\Gamma_{\rm sp}}{2}\rho_{e,e}(v)-\Omega_R{\rm Im}[\tilde\rho_{e,2}(v)]-\Gamma_t\left[\rho_{2,2}(v)-\frac{1}{2}\right], \tag{4b}$$

$$\dot\rho_{e,e}(v)=-\Gamma_{\rm sp}\rho_{e,e}(v)+\Omega_R{\rm Im}[\tilde\rho_{e,1}(v)]+\Omega_R{\rm Im}[\tilde\rho_{e,2}(v)], \tag{4c}$$

$$\dot{\tilde\rho}_{e,1}(v)=-[\Gamma_\perp+i(\delta_{L1}-kv)]\tilde\rho_{e,1}(v)-i\frac{\Omega_R}{2}[\rho_{e,e}(v)-\rho_{1,1}(v)]+i\frac{\Omega_R}{2}\tilde\rho_{2,1}, \tag{4d}$$

$$\dot{\tilde\rho}_{e,2}(v)=-[\Gamma_\perp+i(\delta_{L2}-kv)]\tilde\rho_{e,2}(v)-i\frac{\Omega_R}{2}[\rho_{e,e}(v)-\rho_{2,2}(v)]+i\frac{\Omega_R}{2}\tilde\rho_{1,2}, \tag{4e}$$

$$\dot{\tilde\rho}_{1,2}=-[\Gamma_{\rm coh}+i\delta_R]\tilde\rho_{1,2}-i\frac{\Omega_R}{2}[\tilde\rho_{1,e}-\tilde\rho_{e,2}], \tag{4f}$$

where we have introduced the slowly varying density matrix elements

$$\rho_{e,1}=\tilde\rho_{e,1}e^{-i\omega_{L1}t}, \tag{5a}$$

$$\rho_{e,2}=\tilde\rho_{e,2}e^{-i\omega_{L2}t}, \tag{5b}$$

$$\rho_{2,1}=\tilde\rho_{2,1}e^{-i(\omega_{L2}-\omega_{L1})t}. \tag{5c}$$

Here $\delta_{Li}(v)=\omega_{Li}-\omega_{ei}-kv$ $(i=1,2)$ are the laser detunings, kv is the Doppler shift, and $\delta_R=\delta_{L1}-\delta_{L2}$ is the Raman detuning. The thermal equilibrium population difference between the $|1\rangle$ and $|2\rangle$ sodium hyperfine levels has been neglected in Eqs. (4a) and (4b). The equation for the ground-state coherence does not include any source due to the spontaneous emission process, even if the ground states are degenerated, because in the experimental configuration considered here the two ground states have different quantum numbers. For this case any ground-state coherence created by the spontaneous emission is destroyed in the average over the spontaneous emission angular distribution, as shown in Ref. [9]. On the contrary, that coherence is preserved for two ground states having the same quantum numbers, see Ref. [18].

The steady-state numerical solution of the density matrix equations allows the main features of the coherent-population-trapping phenomenon to be derived. The total fluorescent light intensity I_v emitted from the atoms in the velocity class v is connected to the excited-state population $\rho_{e,e}(v)$ through the following relation:

$$I_v=\rho_{e,e}(v)\Gamma_{\rm sp}. \tag{6}$$

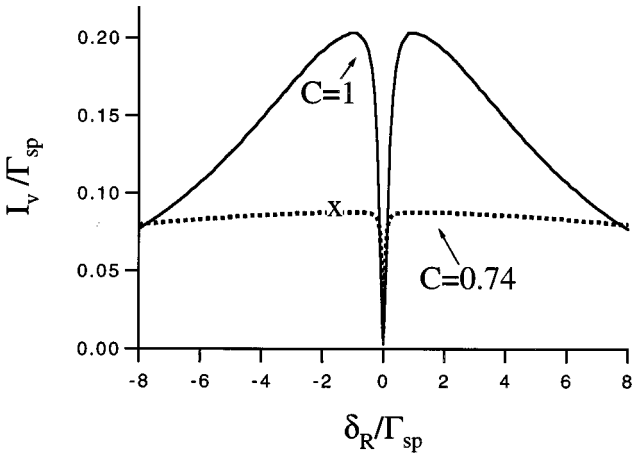

FIG. 3. Numerical results for the fluorescent intensity I_v versus the Raman detuning δ_R, for $\delta_{L1}=0$, $\Omega_R=6\Gamma_{\rm sp}$, and helium pressure of 5 torr. Other parameters as in Fig. 2. The continuous line applies to the $v=0$ atoms, and the dashed line to the atoms with $v=-20\Gamma_{\rm sp}/k$. The data for the dashed line have been multiplied by a factor 5. The contrast C is reported for each case.

Figure 3 reports the fluorescent light intensity I_v versus the Raman detuning δ_R in the case of $\delta_{L1}=0$ and varying the detuning δ_{L2}, for atoms in two different velocity classes, the $v=0$ class and the $v=-20\Gamma_{\rm sp}/k$ class. Similar results are obtained keeping constant the separation between the two laser frequencies and varying the atomic energies through an applied magnetic field, as in the experimental configuration of Ref. [8]. Figure 3 shows that at Raman resonance $\delta_R=0$ the excited-state population and the fluorescent intensity reach a minimum because of the atom accumulation in the coherent-population-trapping superposition. The results for atoms with $v\neq0$ show that at the Raman resonance the coherent-trapping preparation is realized also for atoms not in resonance with the optical transition. For those atoms, a longer time is required to reach the coherent-trapping superposition.

In order to characterize the coherent-population-trapping resonance, a contrast C may be defined as a function of the maximum and minimum in the fluorescence intensity, $I_{\rm max}$ and $I_{\rm min}$, respectively,

$$C=\frac{I_{\rm max}-I_{\rm min}}{I_{\rm max}+I_{\rm min}}. \tag{7}$$

The contrast C depends on the atom-laser interaction parameters and on the relaxation of the ground-state coherence, as analyzed in the next section. For the two velocity classes of Fig. 3, different contrast values are obtained, i.e., $C=1$ for the $v=0$ resonant velocity class and a smaller value for the nonresonant class. In a laser spectroscopy experiment performed within a cell, the fluorescent intensity and the corresponding contrast function are obtained by integration over

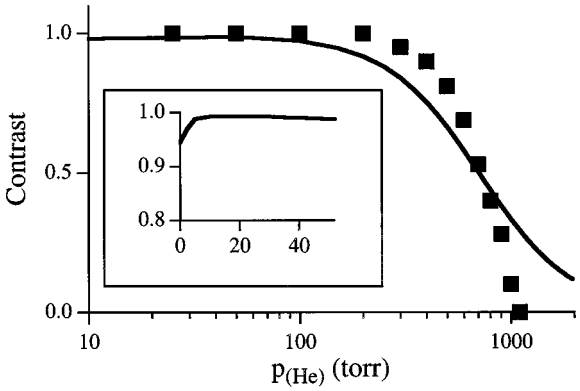

FIG. 4. Experimental results (square points) from Ref. [8] for the contrast C of the coherent-population-trapping resonance versus helium buffer-gas pressure. A 10% accuracy applies to both contrast and pressure values. The continuous line is derived for the contrast within the VCC theoretical treatment, by using $\Gamma^{(1)}_{\mathrm{VCC}}(1-\alpha)=1.2\times10^4\ \mathrm{s}^{-1}\ \mathrm{torr}^{-1}$. The inset shows the theoretical dependence of the contrast at low buffer-gas pressure.

the velocity distribution. Because of the relation between the contrast function and emitted fluorescent light, the resonant atoms with larger excited-state populations and larger fluorescent light intensities (continuous line of Fig. 3) contribute mostly to the velocity-averaged contrast. Experimental results from Ref. [8] for the total contrast function of the sodium atoms versus the helium buffer-gas pressure at constant laser frequencies, $\delta_{L1}=\delta_{L2}=0$, and Rabi frequency $\Omega_R=6\Gamma_{\mathrm{sp}}$, are reported in Fig. 4.

B. Coupled and noncoupled states

The process of coherent-population trapping may be described on the basis of coupled and noncoupled states, $|\mathrm{C}\rangle$ and $|\mathrm{NC}\rangle$, defined in Ref. [9]:

$$|\mathrm{C}\rangle=\frac{1}{\sqrt{2}}[|1\rangle+|2\rangle], \tag{8a}$$

$$|\mathrm{NC}\rangle=\frac{1}{\sqrt{2}}[|1\rangle-|2\rangle]. \tag{8b}$$

These states have Rabi frequency coupling with the excited state $\Omega_R\sqrt{2}$ and 0, respectively. The time evolution of the density matrix elements in the coupled-noncoupled basis is obtained from Eqs. (4) by applying the linear transformation of Eqs. (8). At the Raman resonance, the atomic population is pumped into the noncoupled state, which is not excited by the laser radiation, so that the excited-state population and the emitted fluorescent intensity reach the minimum of Fig. 3.

Under the assumption that the Rabi frequency Ω_R is small compared to Γ_{sp} and $\Gamma_\perp$, the excited-state population is small as compared to those of the ground states, and it may be neglected. Furthermore, on the slow time scale of the evolution for the ground-state populations and coherence, the optical coherences, evolving at the $1/\Gamma_\perp$ time scale, may be adiabatically eliminated. Thus time evolution equations for only the $\rho_{\mathrm{C,C}}(v)$, $\rho_{\mathrm{NC,NC}}(v)$, and $\rho_{\mathrm{C,NC}}(v)$ density matrix elements are obtained. Near the Raman resonance condition $\delta_R=\delta_{L1}-\delta_{L2}\sim0$, the difference between δ_{L1} and δ_{L2} may be neglected, i.e., $\delta_{L1}\sim\delta_{L2}\sim\delta_L$. These equations are then obtained:

$$\frac{d}{dt}[\rho_{\mathrm{C,C}}(v)-\rho_{\mathrm{NC,NC}}(v)]=-2\Gamma'(v)\rho_{\mathrm{C,C}}-\Gamma_{\mathrm{coh}}[\rho_{\mathrm{C,C}}-\rho_{\mathrm{NC,NC}}]-i\delta_R[\rho_{\mathrm{NC,C}}-\rho_{\mathrm{C,NC}}], \tag{9a}$$

$$\frac{d}{dt}[\rho_{\mathrm{NC,C}}(v)-\rho_{\mathrm{C,NC}}(v)]=-(\Gamma_{\mathrm{coh}}+\Gamma'(v)[\rho_{\mathrm{NC,C}}-\rho_{\mathrm{C,NC}}]-i\delta_R[\rho_{\mathrm{C,C}}-\rho_{\mathrm{NC,NC}}]. \tag{9b}$$

The pumping rate from the coupled state, $\Gamma'(v)$, given by

$$\Gamma'(v)=\frac{\Omega_R^2}{2}\frac{\Gamma_\perp}{\Gamma_\perp^2+(\delta_{\mathrm{L}}-kv)^2}, \tag{10}$$

has been defined in laser cooling analyses [9,19], except for the velocity dependence due to the Doppler shift. The dependence of $\Gamma_\perp$ on the helium pressure produces a pressure dependence of the pumping rate, as reported in Fig. 2 for $\Gamma'(0)$.

From the steady-state solution of Eqs. (9), the populations for the noncoupled and coupled states are derived as

$$\rho_{\mathrm{NC,NC}}(v)=\frac{1}{2}\left[1+\frac{\Gamma'(v)}{\delta_{\mathrm{HWHM}}}\frac{1}{1+(\delta_R/\delta_{\mathrm{HWHM}})^2}\right], \tag{11a}$$

$$\rho_{\mathrm{C,C}}(v)=\frac{1}{2}\left[1-\frac{\Gamma'(v)}{\delta_{\mathrm{HWHM}}}\frac{1}{1+(\delta_R/\delta_{\mathrm{HWHM}})^2}\right], \tag{11b}$$

with the δ_{HWHM} half-width at half maximum of the coherent-population-trapping resonance of the atoms having velocity v given by

$$\delta_{\mathrm{HWHM}}=\Gamma'(v)+\Gamma_{\mathrm{coh}}. \tag{12}$$

At the Raman resonance $\delta_R=0$ the population of the noncoupled state reaches a maximum, whereas the population of the coupled state, and thus the fluorescent intensity from the excited state, reaches a minimum value. The fluorescent intensity I_v of Eq. (6) can be expressed as a function of $\rho_{\mathrm{NC,NC}}$ and $\rho_{\mathrm{C,C}}$, and the contrast function $C(v)$ for atoms with velocity v may be derived as

$$C(v)=\frac{1}{1+2\Gamma_{\mathrm{coh}}/\Gamma'(v)}. \tag{13}$$

This expression shows that the contrast function is near its maximum value of 1 if $\Gamma_{\mathrm{coh}}\ll\Gamma'(v)$, and decreases drastically for $\Gamma_{\mathrm{coh}}\sim\Gamma'(v)$. Equation (10) shows that as a function of atomic velocity, the pumping rate is a maximum for atoms having resonant velocity $v_0=\delta_L/k$, and decreases when the velocity is away from this value. By combining the dependence of Γ' on v and the relation between C and Γ',

we obtain a maximum contrast for atomic velocity v_0, and the contrast decreases drastically for velocities such that

$$|v-v_0|\sim\Gamma_\perp\sqrt{\left(\frac{\Omega_R^2}{\Gamma_\perp}\right)^2\frac{\Gamma_\perp}{2\Gamma_{\rm coh}}-1}. \tag{14}$$

Applying this equation to the experimental conditions of Ref. [8], at $\delta_L=0$ and $\Omega_R=6\Gamma_{\rm sp}$, and assuming $\Gamma^p_{\rm coh}=0$, we find that the contrast function remains at the maximum value of 1 for all velocities within the Doppler profile up to the largest buffer-gas pressure examined in Ref. [8], $p\sim10^3$ torr. This result is also obtained by performing an integration of the fluorescent intensity over the velocity distribution. The role played by the $\Gamma^p_{\rm coh}$ collisional damping on the contrast will be analyzed next.

C. Velocity-changing collisions

Velocity-changing collisions which shuffle atoms between different velocity classes, represent another important source of relaxation for the ground state. The $\Gamma_{\rm VCC}$ rate for VCC of ground-state sodium atoms with helium buffer gas is $4.4\times10^7\ p\ {\rm s}^{-1}\ {\rm torr}^{-1}$ [20,15]. Thus the VCC rate, plotted in Fig. 2, is larger than the rates of all other relaxation processes. VCC could modify the atomic velocity without affecting the atomic coherence in the ground state: in this case the atoms prepared by laser radiation in a noncoupled state are transferred to other velocity classes. If this transfer applies with high efficiency, all the atomic velocity classes are pumped into the noncoupled state, either by direct pumping or by VCC. The conservation of optical coherences in VCC has been discussed by Le Gouët and Berman [21]. The Zeeman or hyperfine coherences involved in the sodium noncoupled state should be well preserved in collisional processes because the two atomic states that compose that state belong to the same electronic state, and thus experience the same interatomic potential during a collisional process, as pointed out by de Lignie and Eliel [5].

The influence of VCC on the coherent-population-trapping process is formally treated by writing the density matrix equations for each velocity class and introducing in those equations the probability for VCC between different classes, as in Graf *et al.* [7]. The VCC kernel for sodium atoms colliding with a buffer gas has been derived in Ref. [20], so a numerical solution of the density matrix equations can be performed. A different approach will be used here to describe the combination of VCC and coherent-population trapping. First we note that the collision kernels required to describe the VCC process depend on the angular momentum of the atomic levels, and for the coherent superposition of sodium hyperfine levels a precise modeling of the kernels is quite complex. Instead, we model the three-level system as the $(m_g=-1\rightarrow m_e=0\leftarrow m_g=1)$ Λ system of a $J_g=1\rightarrow J_e=1$ transition, where the VCC process is described in terms of the collisional relaxation rates $\Gamma^{(0)}_{\rm VCC}$ and $\Gamma^{(1)}_{\rm VCC}$ for population and alignment and the associated $K^{(0)}(v'\rightarrow v)$ and $K^{(1)}(v'\rightarrow v)$ collisional kernels [20]. For that three-level system the VCC process is described by the following equations:

$$\frac{d}{dt}[\rho_{1,1}(v)+\rho_{2,2}(v)]=-\Gamma^{(0)}_{\rm VCC}[\rho_{1,1}(v)+\rho_{2,2}(v)]+\int K^{(0)}(v'\rightarrow v)\times[\rho_{1,1}(v')+\rho_{2,2}(v')]dv', \tag{15a}$$

$$\frac{d}{dt}[\rho_{1,1}(v)-\rho_{2,2}(v)]=-\Gamma^{(1)}_{\rm VCC}[\rho_{1,1}(v)-\rho_{2,2}(v)]+\int K^{(1)}(v'\rightarrow v)\times[\rho_{1,1}(v')-\rho_{2,2}(v')]dv', \tag{15b}$$

$$\frac{d}{dt}\rho_{1,2}(v)=-\Gamma^{(1)}_{\rm VCC}\rho_{1,2}(v)+\int K^{(1)}(v'\rightarrow v)\rho_{1,2}(v')dv'. \tag{15c}$$

At this point the transformation to the coupled-noncoupled basis may be applied, so that by combining Eqs. (9) and (15) the complete equations for the density matrix elements in the coupled-noncoupled basis are obtained,

$$\frac{d}{dt}[\rho_{\rm C,C}(v)-\rho_{\rm NC,NC}(v)]=-2\Gamma'(v)\rho_{\rm C,C}-i\delta_R[\rho_{\rm NC,C}-\rho_{\rm C,NC}]-(\Gamma_t+\Gamma^{(1)}_{\rm VCC})\times[\rho_{\rm C,C}-\rho_{\rm NC,NC}]+\int K^{(1)}(v'\rightarrow v)\times[\rho_{\rm C,C}(v')-\rho_{\rm NC,NC}(v')]dv', \tag{16a}$$

$$\frac{d}{dt}[\rho_{\rm NC,C}(v)-\rho_{\rm C,NC}(v)]=-[\Gamma'(v)+\Gamma_t+\Gamma^{(1)}_{\rm VCC}][\rho_{\rm NC,C}-\rho_{\rm C,NC}]-i\delta_R[\rho_{\rm C,C}-\rho_{\rm NC,NC}]+\int K^{(1)}(v'\rightarrow v)\times[\rho_{\rm NC,C}(v')-\rho_{\rm C,NC}(v')]dv'. \tag{16b}$$

These equations involve the collision kernel $K^{(1)}$. In general Eqs. (16), although quite complicated, may be solved using iterative techniques. However, for strong collisions the kernel is greatly simplified and can be approximated by

$$K^{(1)}(v'\rightarrow v)=\alpha\Gamma^{(1)}_{\rm VCC}W(v), \tag{17}$$

where $W(v)$ describes the Maxwell-Boltzmann velocity distribution

$$W(v)=\frac{1}{\sqrt{\pi}ku}e^{-(v/u)^2}, \tag{18}$$

where u is the thermal width and ku is the $1/e$ Doppler width. Furthermore, for rapid VCC coverage of the velocity distribution, the atoms may be assumed to have a thermal

distribution. As discussed in Refs. [10,12], two conditions are required to ensure a rapid velocity coverage: (1) the number of VCC processes occurring during the $1/\Gamma_t$ ground-state relaxation time should be large compared to the total number of homogeneous velocity bins within the Doppler width,

$$\frac{\Gamma_{\rm VCC}}{\Gamma_t} \gg \frac{ku}{\Gamma_\perp}, \tag{19}$$

and (2) the VCC rate should be larger than the pumping rate,

$$\Gamma_{\rm VCC} \gg \Gamma'(v). \tag{20}$$

Under those conditions the thermal distribution of the velocity dependence allows us to write the coupled-noncoupled occupations as

$$\rho_{i,j}(v) = W(v) R_{i,j}, \tag{21}$$

with $(i,j)=$(C,NC). By integrating Eqs. (16) over the velocity distribution and making use of Eqs. (18) and (21), we obtain the following equations for $R_{i,j}$:

$$\frac{d}{dt}[R_{\rm C,C} - R_{NC,NC}] = -2\Gamma'_D R_{\rm C,C} - [\Gamma_t + \Gamma^{(1)}_{\rm VCC}(1-\alpha)] \times [R_{\rm C,C} - R_{\rm NC,NC}] + i\delta_R [R_{\rm NC,C} - R_{\rm C,NC}], \tag{22a}$$

$$\frac{d}{dt}[R_{\rm NC,C} - R_{\rm C,NC}] = -(\Gamma_t + \Gamma^{(1)}_{\rm VCC}(1-\alpha) + \Gamma'_D) \times [R_{\rm NC,C} - R_{\rm C,NC}] + i\delta_R [R_{\rm C,C} - R_{\rm NC,NC}], \tag{22b}$$

where the Doppler integrated pumping rate Γ'_D is defined as

$$\Gamma'_D = \frac{\Omega_R^2}{2\Gamma_\perp} V(ku, \Gamma_\perp), \tag{23}$$

and the Voigt function $V(ku,\Gamma_\perp)$ is given by

$$V(ku,\Gamma_\perp) = \frac{1}{\sqrt{\pi}ku} \int \frac{\Gamma_\perp^2}{\Gamma_\perp^2 + (\delta_L - z)^2} e^{-(z/ku)^2} dz. \tag{24}$$

The steady-state solution of these equations provides the expressions for the total population of the coupled-noncoupled states and their difference

$$R_{\rm NC,NC} - R_{\rm C,C} = \frac{\Gamma'_D}{\delta_{\rm HWHM}} \frac{1}{1 + (\delta_R/\delta_{\rm HWHM})^2}, \tag{25}$$

with the half-width at half maximum given by

$$\delta_{\rm HWHM} = \Gamma_t + \Gamma^{(1)}_{\rm VCC}(1-\alpha) + \Gamma'_D. \tag{26}$$

Thus the total contrast function is

$$C = \frac{1}{1 + 2[\Gamma_t + \Gamma^{(1)}_{\rm VCC}(1-\alpha)]/\Gamma'_D}. \tag{27}$$

The expressions for the occupations of the coupled-noncoupled states and the contrast are very similar to those previously derived for each velocity class. The main differences are that the coherence relaxation includes the $\Gamma^{(1)}_{\rm VCC}(1-\alpha)$ VCC term and that the velocity-dependent pumping rate of Eq. (10) is replaced by the Doppler pumping rate, i.e., a pumping rate of the whole Doppler width treated as homogeneous.

From the rates plotted in Fig. 2 and $ku = 6\times10^9$ s^{-1} in sodium at room temperature, we find that under the experimental conditions of Fig. 4 at helium pressures larger than 100 torr, the conditions of both Eqs. (19) and (20) are well satisfied. Equation (27) may be used to fit the contrast measurements versus helium buffer gas reported in Fig. 4, in order to derive a value for the VCC parameter $\Gamma^{(1)}_{\rm VCC}(1-\alpha)$. The continuous line in Fig. 4 shows the theoretical dependence of the contrast on the buffer gas assuming $\Gamma^{(1)}_{\rm VCC}(1-\alpha) = 1.2\times10^4\ p$ s^{-1} torr^{-1}. Satisfactory agreement with the experimental results is obtained. It must be noted that the theoretical near-Lorentzian line shape for the dependence of the contrast on the buffer-gas pressure cannot provide a perfect fit for the experimental data that present a sharp cut off around 1100 torr. The experimental setup of Refs. [1,8] was based on an inhomogeneous magnetic field to localize in space the coherent-population-trapping resonance. That inhomogeneous magnetic field could have modified the measured maximum fluorescent intensity, and also the dependence of the contrast function on the buffer-gas pressure. Moreover, the Rabi frequency $\Omega_R = 6\Gamma_{\rm sp}$ has been derived from the total laser intensity, but the spatial dependence of the Rabi frequency over the laser Gaussian profile should have been properly treated through an integration over the spatial dependence of the contrast function. The inset to Fig. 4 shows the contrast function at low buffer-gas pressures, a regime not investigated in the experiment of Ref. [8]. In the low pressure region, the contrast function presents a kink associated with the Γ_t modification occurring at those pressure values (see Fig. 2). A similar kink is presented by the contrast function of Eq. (7). Figure 2 shows the expected dependence of the $\delta_{\rm HWHM}$ half-width at half maximum for the coherent-population-trapping resonance, as derived from Eq. (26), by using the VCC collisional rate obtained from the contrast. The decrease of $\delta_{\rm HMHW}$ at large buffer-gas pressure is in agreement with the dependence observed by Xu [8].

From the derived value of the collisional rate of the ground-state coherence and from the $\Gamma_{\rm VCC}$ value of Refs. [20,15], an α value of 0.9997 is obtained. This large value indicates the large probability of sodium atoms to experience collisions with helium gas preserving the ground-state coherence. The present value for the VCC depolarization collisional rate, and the corresponding cross section 2×10^{-18} cm^2, is smaller than the cross section for VCC population transfer in sodium reported in Ref. [15]. However, the derived cross section is quite large when compared to the typical values for the depolarizing collisions between alkali metals and rare gases, see Ref. [16]. The reason for this disagreement may be associated to the several simplifying assumptions introduced in the theoretical analysis, such as that of strong collisions or of a reduction of the whole sodium ground-state structure to a two-level system.

III. CONCLUSIONS

This work analyzes the relaxation processes of the ground-state superposition created in coherent-population trapping. The role of velocity-changing collisions in redistributing the coherent superposition between different velocity classes has been evidenced. The VCC relaxations have been analyzed within the assumption of strong collisions. The preparation of a whole inhomogeneous atomic sample in the coherent superposition of states may be achieved using a large Rabi frequency, so that nonresonant atoms also are pumped into the coherent superposition, as reported in Fig. 3. Alternatively, for a small Rabi frequency the velocity-changing collisions may be used to transfer the coherent superposition from one velocity class to other ones.

The value derived here for the VCC collisional rate of the ground-state coherence should be considered only as an order of magnitude. That value has been derived from a fit of the only available data set. Measurements taken at different laser intensities could provide a consistency check of the theoretical analysis. In the fit, the laser detunings were assumed to be zero, i.e., both lasers were assumed resonant with the $v=0$ velocity, but that detuning was not precisely measured in the experiment of Ref. [8]. The laser beams have been assumed to have polarizations such as to induce transitions within a close three-level system. On the contrary, weak wrong polarization components were present in the experimental configuration. Those components could induce undesired transitions to other levels, as examined in Ref. [7] for the laser-without-inversion experiments of Ref. [6]. A rough estimate indicates that this process has a negligible influence on the dependence of the contrast on the buffer-gas pressure.

From the experimental point of view, a direct measurement of the VCC coherence transfer can be obtained using the four-laser scheme of Maichen *et al.* [22]. Thus two lasers should be used to prepare the atomic coherent superposition, and two additional lasers shifted in their absolute frequency but with their frequency difference matching the ω_{12} ground-state splitting should probe the coherence as a function of atomic velocity. From a theoretical point of view, the description of the collisions through a strong collision kernel, introduced here as in Refs. [10–14], is certainly quite inaccurate for the case of sodium-helium collisions, even if the results at high pressure may not be overly sensitive to the form of the kernel. A numerical solution of the density matrix equations and a numerical integration over the velocity distribution could be used to derive the precise form of the collisional kernel. Other important processes, such as, for instance, the relaxation of the excited state, may also be included in that analysis. However, the aim of the present analysis is to point out through a rough description the information to be derived from the study of the coherent-population-trapping phenomenon in the presence of collisional processes. In effect, the equations derived here for the contrast function provide an accurate indication for the amount of coherent-population trapping formed under different conditions of a three-level system.

In the applications of coherent-population trapping to laser cooling [9,23,4], the atomic density is low, so that the relaxation rates previously discussed are very small. Under these conditions the interaction between the atoms is not the relevant mechanism for the ground-state coherences. The important process for the destruction of the ground-state coherent superposition is the atomic absorption of photons not belonging to the modes of the E_{L1} and E_{L2} electric fields defining the coherent superposition. Even if the applied electric fields contain only photons in the E_{L1} and E_{L2} modes, photons having the same frequency but different propagation directions are produced by spontaneous emission from the $|e\rangle$ excited state in the phase of preparation of the noncoupled coherent superposition. Those photons, if absorbed by atoms already prepared in the noncoupled coherent superposition, destroy the ground-state superposition. For the laser cooling based on the coherent-population trapping, the reabsorption of the spontaneously emitted light is the relaxation process of coherent-population trapping. The reabsorption rate depends on the photons emitted in the preparation phase of the coherent-population trapping and on the specific geometry of the laser cooling experiment. An upper limit of the reabsorption coherence relaxation rate will be obtained supposing two separate and identical samples, containing N atoms, the first one already prepared in the coherent-population trapping, and the second one not prepared in the coherent-population trapping, whose emitted photons produce a relaxation for the ground-state coherence of the first sample. In the first sample, the number n_{sp} of photons emitted by spontaneous emission per unit time is $n_{\mathrm{sp}}=N\Gamma\Omega_R^2/2(\delta_L^2+\Gamma_{\mathrm{sp}}^2/4+\Omega_R^2)$. The damping rate of the ground-state coherence is given by the absorption rate of the emitted photons. By supposing that all the photons from the second sample reach the first sample, i.e., that the photons do not escape out of the regions containing the atoms, the reabsorption rate is equal to $\lambda^2 c n_{\mathrm{sp}}/2$. At an atomic density $N=10^8$ cm^{-3}, the reabsorption relaxation rate of the coherence is around 10^{-2} s^{-1} and this rate increases with the atomic number. Such a rate, even if smaller than the collisional relaxation rates examined in this work, is quite important for the efficiency of the laser cooling process based on the coherent-population trapping. However, the precise value of the reabsorption coherence rate depends on the preparation of the atoms in the coherent-population-trapping state. It should be noticed that for large values of the atomic density the reabsorption coherence relaxation rate becomes comparable to the collisional relaxation rate. Thus the role of the reabsorption relaxation should also be carefully investigated in future experiments.

ACKNOWLEDGMENTS

The author wishes to thank M. Lukin, D. Nikonov, M.O. Scully, and J.H. Xu for useful discussions. The author gratefully acknowledges support from the JILA Visiting Fellowship Program.

[1] G. Alzetta, A. Gozzini, L. Moi, and G. Orriols, Nuovo Cimento B **36**, 5 (1976); G. Alzetta, L. Moi, and G. Orriols, *ibid.* **52**, 205 (1979).

[2] E. Arimondo and G. Orriols, Lett. Nuovo Cimento **17**, 333 (1976); G. Orriols, Nuovo Cimento B **53**, 1 (1979).

[3] H. R. Gray, R. M. Whitley, and C. R. Stroud, Jr., Opt. Lett. **3**, 218 (1978).

[4] E. Arimondo, in *Progress in Optics*, edited by E. Wolf, (Elsevier, Amsterdam, 1996), Vol. 35, p. 257.

[5] M. C. de Lignie and E. R. Eliel, Opt. Commun. **72**, 205 (1989); E. R. Eliel, Adv. At. Mol. Phys. **30**, 199 (1993).

[6] E. S. Fry, X. Li, D. Nikonov, G. G. Padmabandu, M. O. Scully, A. V. Smith, F. K. Tittel, C. Wang, S. R. Wilkinson, and S. Y. Zhu, Phys. Rev. Lett. **70**, 3235 (1993); D. E. Nikonov, U. W. Rathe, M. O. Scully, S. Y. Zhu, E. S. Fry, X. Li, G. G. Padmabandu, and M. Fleischhauer, Quantum Opt. **6**, 245 (1994).

[7] M. Graf, E. Arimondo, E. S. Fry, M. O. Scully, D. Nikonov, and G. G. Padmabandu, Phys. Rev. A **51**, 4030 (1995).

[8] J. H. Xu, Ph.D. thesis, Scuola Normale Superiore, Pisa, Italy, 1994 (unpublished).

[9] A. Aspect, E. Arimondo, R. Kaiser, N. Vansteenkiste, and C. Cohen-Tannoudji, Phys. Rev. Lett. **61**, 826 (1988); J. Opt. Soc. Am. B **6**, 2112 (1989).

[10] R. Walkup, A. Spielfiedel, W. D. Phillips, and D. E. Pritchard, Phys. Rev. A **23**, 1869 (1981).

[11] P. G. Pappas, R. A. Forber, W. W. Quivers, Jr., R. R. Dasari, M. S. Feld, and D. E. Murnick, Phys. Rev. Lett. **47**, 236 (1981).

[12] W. W. Quivers, Jr., Phys. Rev. A **24**, 3822 (1986).

[13] G. Shimkaveg, W. W. Quivers, Jr., R. R. Dasari, and M. S. Feld, Phys. Rev. A **48**, 1409 (1993).

[14] F. de Tomasi, M. Allegrini, E. Arimondo, G. S. Agarwal, and P. Ananthalakshmi, Phys. Rev. A **48**, 3820 (1993).

[15] H. G. C. Werij and J. P. Woerdman, Phys. Rep. **169**, 146 (1988), and references therein.

[16] W. Happer, Rev. Mod. Phys. **44**, 169 (1972).

[17] In Ref. [11] the escape rate Γ_t, defined for the case of a laser beam with radius R smaller than the cell radius, depends on both laser and cell radii. However, for the experimental conditions of Ref. [8], that correction to Eq. (2) is negligible.

[18] J. Javanainen, Europhys. Lett. **17**, 407 (1992).

[19] J. Dalibard and C. Cohen-Tannoudji, J. Opt. Soc. Am. B **6**, 2023 (1989); P. Marte, R. Dum, R. Taïeb, P. Zoller, M. S. Shahriar, and M. Prentiss, Phys. Rev. A **49**, 4826 (1994).

[20] P. R. Berman, J. E. M. Haverkort, and J. P. Woerdman, Phys. Rev. A **34**, 4647 (1986); J. E. M. Haverkort, J. P. Woerdman, and P. R. Berman, *ibid.* **36**, 5251 (1987).

[21] J. L. Le Gouët and P. Berman, Phys. Rev. A **17**, 52 (1978).

[22] W. Maichen, R. Gaggl, E. Korsunsky, and L. Windholz, Europhys. Lett. **31**, 189 (1995).

[23] J. Lawall, F. Bardou, B. Saubamea, K. Shimizu, N. Bigelow, M. Leduc, A. Aspect, and C. Cohen-Tannoudji, Phys. Rev. Lett. **61**, 826 (1994); J. Lawall, S. Kulin, B. Saubamea, N. Bigelow, M. Leduc, and C. Cohen-Tannoudji, *ibid.* **75**, 4194 (1995).